

## MHD Flow of a Non-Newtonian Power Law Fluid over a Vertical Stretching Sheet with the Convective Boundary Condition

Azeem SHAHZAD<sup>1,\*</sup> and Ramzan ALI<sup>1,2</sup>

<sup>1</sup>Department of Mathematics, Quaid-I-Azam University, Islamabad 44000, Pakistan

<sup>2</sup>University of Central Asia, Bishkek 720001, Kyrgyz Republic

(\*Corresponding author's e-mail: azeemhaadi@yahoo.com)

Received: 22 April 2012, Revised: 2 June 2012, Accepted: 13 December 2012

### Abstract

In this article, we study the power law model of steady state, viscous, incompressible MHD flow over a vertically stretching sheet. Furthermore, heat transfer is also addressed by using the convective boundary conditions. The coupled partial differential equations are transformed into ordinary differential equations (ODEs) using similarity transformations. The transformed highly non-linear ODEs are solved by using the Homotopy Analysis Method (HAM). The influence of different parameters on the velocity and temperature fields are analyzed and discussed.

**Keywords:** Power law model, heat transfer, convective boundary conditions, vertical stretching sheet

### Introduction

In the recent decades, the investigation of the flow and heat transfer of a non-Newtonian fluid has gained considerable attention because of its extensive engineering applications. As a subclass of non-Newtonian fluid, the power-law model is found to be good in representing the pseudo-plastic and dilatant behavior of the fluid. It is frequently used in oil-engineering. In the existing literature a masterpiece of work has been done on heat and mass transfer of power-law fluid. Schowalter [1] was the first one, who studied the application of a boundary layer to power law pseudo-plastic fluids. Acrivos [2] investigated the steady laminar flow of non-Newtonian fluid over a plate. Their work was extended to find similarity solutions for non-Newtonian power law fluids by Lee and Amen [3]. Cran [4] gave an exact similarity solution in closed analytical form for boundary layer flow of a viscous fluid over a stretching sheet. Anderson and Dandapat [5] discussed the non-Newtonian power law fluid over a linearly stretching sheet. Parasad *et al.* [6] investigated the hydromagnetic flow and heat transfer of a non-Newtonian power-law fluid over a vertical stretching sheet. Shahzad and Ali [7] put forward the analytic solution of the power-

law fluid over the same geometry. Numerous excellent work on the boundary layer flow of non-Newtonian fluids are now available.

Heat transfer of the fluid has tremendous industrial applications for the thermal and moisture treatment of materials, cooling of fibers, paper production and metallurgical processes. Makinde and Aziz [8] analyzed the mixed convection from a convectively heated vertical plate to a fluid with internal heat generation. Khan and Pop [9] studied flow and heat transfer over a continuously moving flat plate in a porous medium. Fox *et al.* [10] studied the continuous moving flat plate with heat transfer and Pal [11] examined the combined effects of non-uniform heat transfer and thermal radiation on unsteady stretching permeable surface. Several authors [12-17] investigated heat transfer of the power-law fluid of various physical problems. In recent decades, several industrial processes have dealt with power law fluid flow with magnetic fields. In this respect, some researchers have advanced this area.

To the best of authors' knowledge, the convective boundary condition of vertical stretching sheet phenomena has not been applied

in the literature. The objective of this article is to investigate the effects of MHD, mixed convections by introducing the convective heat transfer associated with the hot fluid on the other surface of the vertical stretching sheet. This flow phenomenon has several applications in technological processes. In particular, the extrusion of polymer in a melt-spinning process, extruded from the die is generally drawn and stretched into a sheet, then solidified via gradual cooling by direct contact with water. This article is the extension of the work of Parasad *et al.* [6] in which they discussed hydromagnetic flow and heat transfer of the power law model over a vertical stretching sheet. They solved the problem by using the Keller-Box method. In the present paper, we examine and extend the aforementioned paper to give the analytic solution of the MHD power law model of a stretching sheet with the convective boundary condition. We do so with the Homotopy analysis method [18-23].

### Problem formulation and governing equations

Let us consider the steady state, incompressible, mixed convection boundary layer flow of an electrically conducting, power-law fluid in the presence of a transverse magnetic field in a vertically stretching sheet with convective boundary conditions. The induced magnetic field is neglected. Consider the origin is fixed, the positive  $x$ - axis is along the direction of the flow and the  $y$ - axis is measured normal to the sheet. The bottom surface of the sheet is heated by convection from a hot fluid at  $T_f$  which provides a heat transfer coefficient  $h$ . The flow phenomenon is generated as a result of linear stretching of the sheet. We assumed the continuous linear stretching velocity's of the form,  $U(x) = ax$ , where  $a$  is the linear stretching constant,  $x$  is the distance from origin. As illustrated in **Figure 1**.

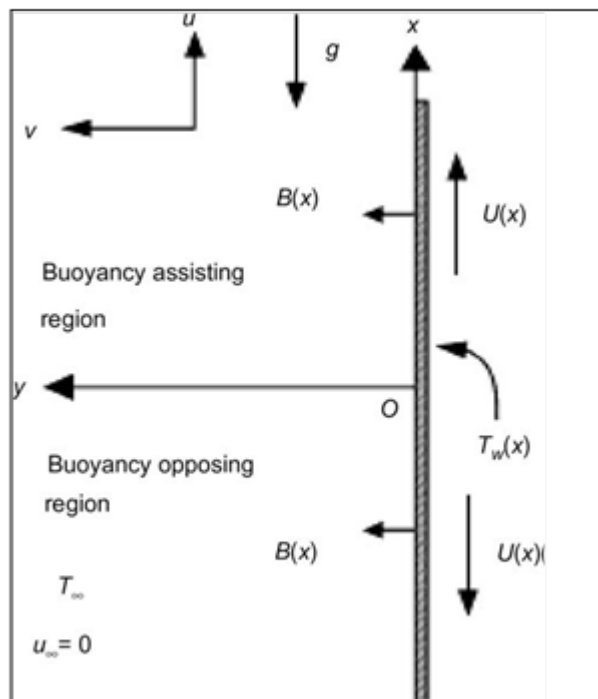


**Figure 1** Physical model of the flow.

Under the boundary layer approximation, the continuity, momentum and energy equations are given by

$$\frac{\partial u}{\partial x} + \frac{\partial v}{\partial y} = 0, \quad (1)$$

$$u \frac{\partial u}{\partial x} + v \frac{\partial u}{\partial y} = -\frac{k}{\rho} \frac{\partial}{\partial y} \left( -\frac{\partial u}{\partial y} \right)^n - \frac{\sigma B_0^2}{\rho} u \pm g\beta(T - T_\infty), \quad (2)$$

$$u \frac{\partial T}{\partial x} + v \frac{\partial T}{\partial y} = \alpha \frac{\partial^2 T}{\partial y^2}. \quad (3)$$

In the above equations,  $u$  and  $v$  are the velocity components along the  $x$  and  $y$  -axes, respectively,  $n$  is the power-law index,  $k$  is the consistency index,  $B_0$  is induced magnetic field,  $\rho$  the density of the fluid,  $\sigma$  is the charge density,  $g$  is the acceleration due to gravity,  $\beta$  is the thermal expansion coefficient,  $T$  is the temperature of the fluid,  $\alpha$  is the thermal conductivity of the fluid. Viscous dissipation is not accounted. In Eq. (2), the first term on the right hand side is the shear rate and is assumed to be negative throughout the boundary layer. Also, the velocity component decreases with the distance  $y$  for a continuous stretching surface. In the present context no pressure gradient is exerted. Instead, the flow is driven solely by a flat surface which moves with a velocity  $U(x)$ . The last term on the right hand side represents the influence of thermal buoyancy force on the flow field, where  $+$  indicates buoyancy assisting and  $-$  for buoyancy opposing the flow, respectively. The buoyancy assisting is represented in the positive  $x$ - axis, which is vertically upward in the flow direction and buoyancy opposing is in the downward direction, in this case the stretching induced flow and the thermal buoyancy flow balance each other. The applicable boundary conditions of the flow are:

$$u(x, y) = U(x) = ax, \quad v(x, y) = 0, \quad (4)$$

$$-k \frac{\partial T}{\partial y} = h(T_f - T) \text{ as } y = 0,$$

$$u(x, y) \rightarrow 0, \quad T(x, y) \rightarrow T_\infty \text{ at } y \rightarrow \infty. \quad (5)$$

Eq. (5) implies that the velocity and temperature vanish outside the boundary layer. Eq. (4) assures the convective boundary condition, where  $h$  is the heat transfer coefficient, which plays an essential role for convection along the boundary, from ambient hot fluid.

We introduce the following dimensionless quantities [6,7].

$$\eta = \frac{y}{x} (\text{Re}_x)^{\frac{1}{n+1}},$$

$$\psi(x, y) = Ux (\text{Re}_x)^{\frac{-1}{n+1}} f(\eta), \quad (6)$$

$$\theta(\eta) = \frac{T - T_\infty}{T_f - T_\infty} \text{ and } T_f = T_\infty + A \left( \frac{x}{l} \right),$$

where  $\eta$  is the similarity transformation variable,  $\text{Re}$  is the Reynolds number,  $\psi(x, y)$  is the stream function,  $f$  and  $\theta$  are the dimensionless similarity function related to the velocity and temperature profiles, respectively.  $T_\infty$  is the temperature of the ambient fluid,  $A$  is a constant whose value depends up on the properties of the fluid,  $x$  is distance from origin and  $l$  is the characteristic length.

The velocity component in terms of stream functions are defined as

$$u = \frac{\partial \psi}{\partial y}, \quad v = -\frac{\partial \psi}{\partial x}. \quad (7)$$

The local Reynolds number is defined as

$$\text{Re}_x = \frac{\rho U^{2-n} x^n}{k}. \quad (8)$$

The conservation of mass i.e. Eq. (1) is satisfied automatically, using the similarity transformation of the momentum and energy

equations with respective boundary conditions taking the following forms

$$n(-f''(\eta))^{n-1} f'''(\eta) - f'^2(\eta) + \left(\frac{2n}{n+1}\right) f(\eta) f''(\eta) - Mf'(\eta) + \lambda\theta(\eta) = 0, \tag{9}$$

$$\theta''(\eta) + \text{Pr} \begin{pmatrix} \frac{2n}{n+1} f(\eta) \theta'(\eta) \\ -f'(\eta) \theta(\eta) \end{pmatrix}, \tag{10}$$

$$f(\eta) = 0, f'(\eta) = 1, \theta'(\eta) = -\gamma[1 - \theta(\eta)] \text{ at } \eta = 0, \tag{11}$$

$$f'(\eta) = \theta(\eta) = 0 \text{ as } \eta \rightarrow \infty, \tag{12}$$

where  $M = 2\sigma B_0 / \rho a$  is the magnetic parameter,  $\lambda = \pm Gr_x / Re_x$  is the buoyancy or mixed convection parameter,  $\text{Pr} = \frac{\alpha^2}{\alpha} (Re_x)^{\frac{2}{n+1}}$  is the modified Prandtl number for power law fluid and  $Gr_x = g\beta(T_f - T_\infty)\rho x a^{-n} / k$  is the local Grashof number. It is important to mention that  $\lambda > 0$  and  $\lambda < 0$  represent the assisting and opposing flows, respectively, while  $\lambda = 0$ , corresponds to the case when the buoyancy force is totally absent. If  $\lambda$  is of order greater than one, the buoyancy forces will dominant the flow, which indicates free convection

$$\gamma = \frac{hx}{k^* Re^{1/n+1}}. \tag{13}$$

For the energy equation to have a similarity solution, the quantity  $\gamma$  must be independent of  $x$ . Consequently, the heat transfer coefficient,  $h_f$ , is proportional to  $x^{-1/n+1}$  and we assume  $h_f = h cx^{-1/n+1}$ , and get

$$h_f = h cx^{-1/n+1}, \tag{14}$$

$$\gamma = \frac{c}{k^*} \left[ \frac{U^{2-n}}{\nu} \right]^{1/n+1}, \tag{15}$$

as the Biot number with  $c$  as an arbitrary constant. We note that when  $\gamma \rightarrow \infty$ , the present problem reduces to the classical boundary layer flow on the stretching sheet with a constant surface temperature.

The local Nusselt number  $Nu_x = q_w x / k^* (T_f - T_\infty)$  with  $q_w$  as the surface heat flux may be found in terms of the dimensionless temperature at the stretched surface

$$Nu_x = Re_x^{-1/2} Nu = -\theta'(0). \tag{16}$$

**The HAM solutions**

According to Eqs. (9) - (10) and boundaries conditions (11) - (12) the solutions for the velocity and temperature fields can be expressed in the form of the following homotopy series

$$f(\eta) = \sum_{i=0}^{\infty} \sum_{j=0}^{\infty} a_{i,j} \eta^i \exp(-j\eta), \tag{17}$$

$$\theta(\eta) = \sum_{i=0}^{\infty} \sum_{j=0}^{\infty} b_{i,j} \eta^i \exp(-j\eta), \tag{18}$$

where  $a_{i,j}$  and  $b_{i,j}$  are the coefficients. Here we choose the initial guesses and auxiliary linear operators in the following forms:

$$f_0(\eta) = 1 - e^{-\eta}, \tag{19}$$

$$\theta_0(\eta) = \frac{\gamma e^{-\eta}}{1 + \gamma}, \tag{20}$$

$$\mathcal{L}_f[\hat{f}(\eta, p)] = \frac{\partial^3 \hat{f}(\eta, p)}{\partial \eta^3} - \frac{\partial \hat{f}(\eta, p)}{\partial \eta}, \tag{21}$$

$$\mathcal{L}_\theta[\hat{\theta}(\eta, p)] = \frac{\partial^2 \hat{\theta}(\eta, p)}{\partial \eta^2} - \hat{\theta}(\eta, p). \tag{22}$$

**Zeroth order deformation**

With the help of the above definitions, we construct the zero-order deformation problems as follows:

$$(1-p)\mathcal{L}_f[\hat{f}(\eta, p) - f_0(\eta)] = p\hbar N_f[\hat{f}(\eta, p)], \tag{23}$$

$$(1-p)\mathcal{L}_\theta[\hat{\theta}(\eta, p) - \theta_0(\eta)] = p\hbar N_\theta[\hat{\theta}(\eta, p), \hat{f}(\eta, p)], \tag{24}$$

$$\hat{f}(\eta, p) = \hat{f}'(\eta, p) = 0 \text{ and } \hat{\theta}(\eta, p) = 1 \text{ at } \eta = 0, \tag{25}$$

$$\begin{aligned} \hat{f}(\eta, p) &= \hat{f}(\eta, p) = 0, \\ \hat{f}'(\eta, p) &= 1 \text{ and } \\ \hat{\theta}(\eta, p) &= -\gamma[1 - \hat{\theta}(\eta, p)] \text{ at } \eta = 0, \end{aligned} \tag{26}$$

$$\hat{f}'(\eta, p) = \hat{\theta}(\eta, p) = 0 \text{ as } \eta \rightarrow \infty, \tag{27}$$

where

$$\begin{aligned} N_f[\hat{f}(\eta, p)] &= \\ n(-\hat{f}''(\eta, p))^{n-1} \hat{f}''(\eta, p) & \\ - \hat{f}'^2(\eta, p) + \left(\frac{2n}{n+1}\right) \hat{f}(\eta, p) \hat{f}''(\eta, p) & \\ - M\hat{f}'(\eta, p) + \lambda \hat{\theta}(\eta, p), & \end{aligned} \tag{28}$$

$$\begin{aligned} N_\theta[\hat{\theta}(\eta, p), \hat{f}(\eta, p)] &= \hat{\theta}''(\eta, p) \\ + \text{Pr} \left( \begin{aligned} &\frac{2n}{n+1} \hat{\theta}'(\eta, p) \hat{f}(\eta, p) \\ & - \hat{\theta}(\eta, p) \hat{f}'(\eta, p) \end{aligned} \right) \end{aligned} \tag{29}$$

here  $p \in [0,1]$  is an embedding parameter and  $\hbar$  the non-zero convergence control parameter.

$$\hat{f}(\eta, 0) = f_0 \text{ and } \hat{\theta}(\eta, 0) = \theta_0, \tag{30}$$

$$\hat{f}(\eta, 1) = f(\eta) \text{ and } \hat{\theta}(\eta, 1) = \theta(\eta). \tag{31}$$

As  $p$  increases from 0 to 1,  $\hat{f}(\eta; p)$  and  $\hat{\theta}(\eta; p)$  vary from  $f_0(\eta)$ ,  $\theta_0(\eta)$  to  $f(\eta)$  and  $\theta(\eta)$ , respectively.

**mth order deformation**

Using Taylor's theorem, we can write

$$\hat{f}(\eta; p) = f_0(\eta) + \sum_{m=1}^{\infty} f_m p^m, \tag{32}$$

$$\hat{\theta}(\eta; p) = \theta_0(\eta) + \sum_{m=1}^{\infty} \theta_m p^m, \tag{33}$$

where

$$f_m(\eta) = \frac{1}{m!} \left. \frac{\partial^m \hat{f}(\eta, p)}{\partial \eta^m} \right|_{p=0}, \tag{34}$$

$$\theta_m(\eta) = \frac{1}{m!} \left. \frac{\partial^m \hat{\theta}(\eta, p)}{\partial \eta^m} \right|_{p=0}. \tag{35}$$

The convergence of the series (32) and (33) is strongly dependent up on  $\hbar$ . Assuming that  $\hbar$  is chosen so that the above series are convergent at  $p = 1$  then from Eqs. (32) and (33) we have

$$f(\eta) = f_0(\eta) + \sum_{m=1}^{\infty} f_m(\eta), \tag{36}$$

$$\theta(\eta) = \theta_0(\eta) + \sum_{m=1}^{\infty} \theta_m(\eta). \tag{37}$$

Differentiating the zero-order deformation problems  $m$ -times with respect to  $p$  and dividing by  $m!$  and setting  $p = 0$ , we get the  $m$ th-order deformation problems of the forms

$$\mathcal{L}_f[f_m(\eta) - f_{m-1}(\eta)] = \hbar_f R^f_m(\eta), \tag{38}$$

$$\mathcal{L}_\theta[\theta_m(\eta) - \theta_{m-1}(\eta)] = \hbar_\theta R^\theta_m(\eta), \tag{39}$$

respective boundary conditions

$$f_m(\eta) = f'_m(\eta) = 0, \text{ and} \tag{40}$$

$$\theta_m(0) = 0 \text{ at } \eta = 0,$$

$$f'_m(\eta) = \theta_m(\eta) = 0 \tag{41}$$

as  $\eta \rightarrow \infty,$

where

$$R_m^f(\eta) = \lambda \theta_{m-1} - M f'_{m-1} \tag{42}$$

$$- \sum_{k=0}^{m-1} f'_{m-1-k} f'_k + \phi_f,$$

$$R_m^\theta(\eta) = \theta''_{m-1} \tag{43}$$

$$- \text{Pr} \sum_{k=0}^{m-1} \theta_{m-1-k} f'_k + \text{Pr} \phi_\theta,$$

and

$$\phi_f = f''_m + \sum_{k=0}^{m-1} f'_{m-1-k} f'_k, \tag{44}$$

$$n = 1$$

$$= -2 \sum_{k=0}^{m-1} f'_{m-1-k} f'_k + \frac{4}{3} \sum_{k=0}^{m-1} f_{m-1-k} f''_k,$$

$$n = 2$$

$$\phi_\theta = \sum_{k=0}^{m-1} \theta'_{m-1-k} f'_k, \tag{45}$$

$$n = 1$$

$$= \frac{4}{3} \sum_{k=0}^{m-1} \theta'_{m-1-k} f'_k. \tag{45}$$

$n = 2$   
The linear non-homogeneous problems (38) - (41) can be solved by using any symbolic computational software like MATHEMATICA in the order  $m = 1, 2, 3, \dots$ .

**Convergence of the series solutions**

The convergence of the series solution is solely dependent upon the value of the auxiliary parameter  $\hbar$ . It is straight forward to choose an appropriate range for  $\hbar$ , which is a horizontal line segment, used to ensure the converge of the HAM solution. In **Figure 2**, the  $\hbar$ -curve of the velocity and temperature has been shown. These figures depict the convergence of the HAM solutions for the range  $-1.7 \leq \hbar_f \leq -0.5$  and  $-1 \leq \hbar_f \leq -0.2$  of the velocity field for  $n = 1$  and  $n = 2$ , respectively. The solution for the temperature converges for  $-1.9 \leq \hbar_\theta \leq -0.5$  and  $-2 \leq \hbar_\theta \leq -0.4$ , for  $n = 1$  and  $n = 2$ , respectively. Also the norm 2 error of two consecutive approximations with HAM is calculated by

$$\sqrt{\frac{1}{21} \sum_{i=0}^{20} [f_{20}(i/20)]^2}$$

to find the best value of  $\hbar$  for which the error is minimum, plotted in **Figures 3** and **4**. These figures depict errors for the various values of the power-index  $n$ .

The  $\hbar$ -curves of  $f''(0)$  for the 20th order approximation when  $\gamma = 1, \lambda = 1, M = 1$  are fixed.

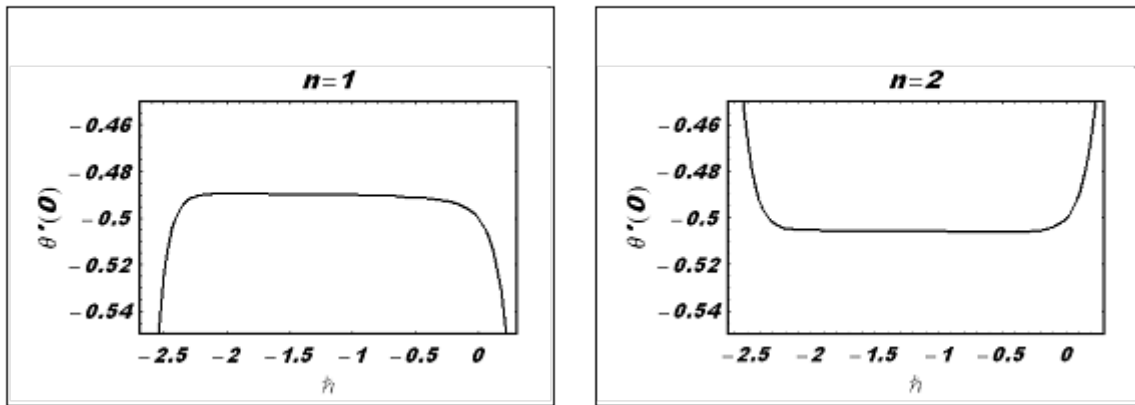


Figure 2 The  $\hat{h}$ -curves of  $\theta'(0)$  for the 20th order approximation when  $\gamma = 1$ ,  $\lambda = 1$ ,  $M = 1$  and  $Pr = 1$  are fixed.

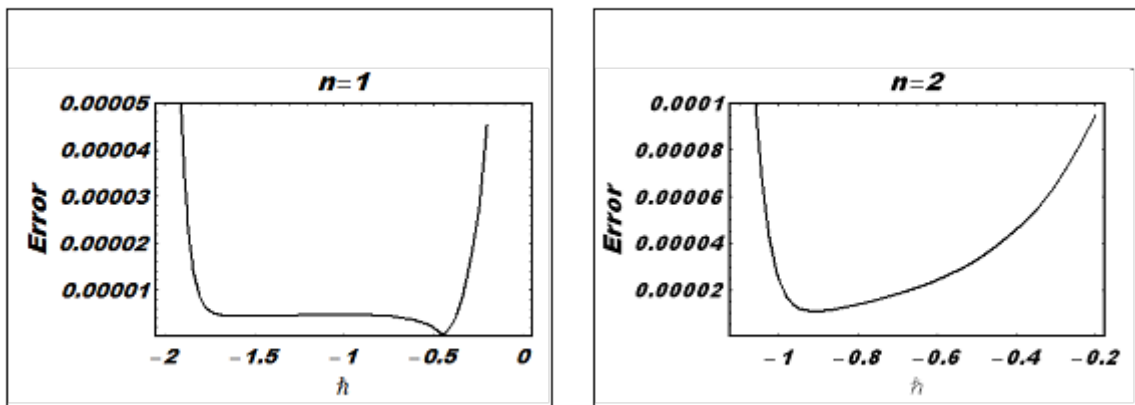
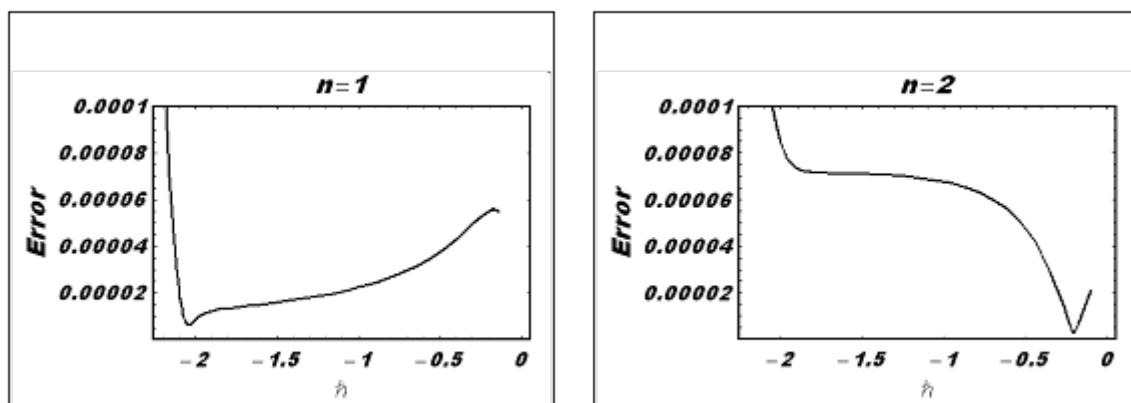


Figure 3 The error of norm 2 for the 20th order approximation by Homotopy analysis method for  $f(\eta)$ .



**Figure 4** The error of norm 2 for the 20th order approximation by Homotopy analysis method for  $\theta(\eta)$ .

### Graphical discussion

In order to observe the influence of the power index,  $n$ , and other parameters on the velocity profiles they have been plotted in **Figures 5 - 7**. In **Figure 5**, we draw the effects of the magnetic parameter on the velocity profile for different values of power-index,  $n$ . From this figure it is clear that with an increase in the magnetic parameter,  $M$ , the velocities for both  $n=1$  and  $n=2$ , decrease. Also the boundary layer thickness decreases with an increase in the magnetic parameter,  $M$ . **Figure 6** shows the effects of the Prandtl number,  $Pr$ , on the velocity profile. A similar behavior to that of the magnetic parameter is observed. **Figure 7** is plotted to examine the influence of the convection parameter,  $\lambda$ , on the velocity profile. From these figures it is observed that the velocity profile and, hence, the boundary layer thickness increase with an increase in the convection parameter  $\lambda$ .

**Figures 8 - 11** are plotted in order to see the significant effects of the different pertinent

parameters on the temperature profiles. **Figure 8** shows the effects of the magnetic parameter  $M$  on the temperature profile. This figure shows that with an increase in  $M$ , temperatures and the thermal boundary layer thickness increase. From **Figure 9** it is clear that with the increase in the Prandtl number, the temperature profile decreases for different values of the power-law index,  $n$ . **Figure 10** shows the influence of the convection parameter  $\lambda$  on the temperature field with an increase in the value of  $\lambda$ , the temperatures decrease. In **Figure 11** the effects of the Biot number are plotted, from this figure it is observed that with an increase in  $\gamma$ , the temperatures increase.

The values of the Nusselt number are recorded in **Table 1** for different values of the governing parameters. It is observed that the heat transfer rate increases with an increase in the values of  $n$ ,  $\lambda$ ,  $Pr$  and  $\gamma$ , except for the magnetic parameter  $M$  for which it decreases.

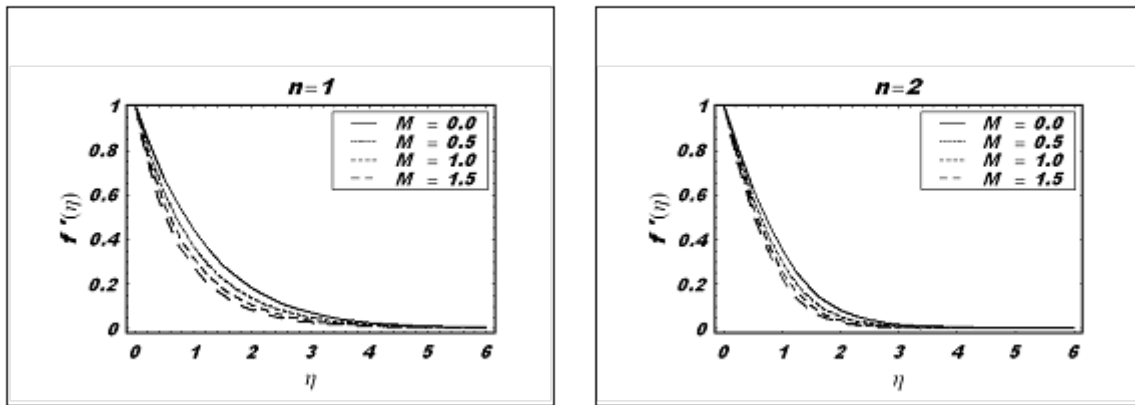


**Figure 5** The influence of the magnetic parameter,  $M$ , on the velocity profiles when  $Pr = 1$ ,  $\lambda = 1$  and  $\gamma = 1$  are fixed.

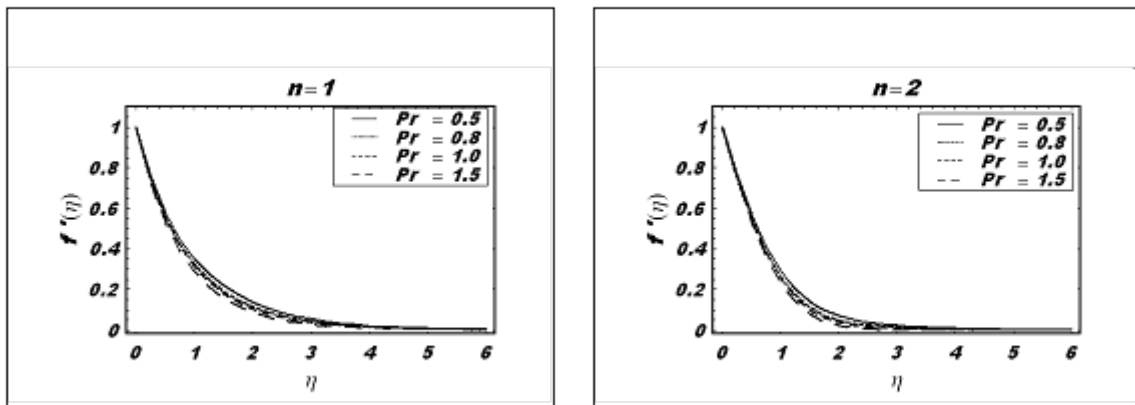


**Figure 6** The influence of the Prandtl number,  $Pr$ , on the velocity profiles when  $M = 1$ ,  $\lambda = 1$  and  $\gamma = 1$  are fixed.

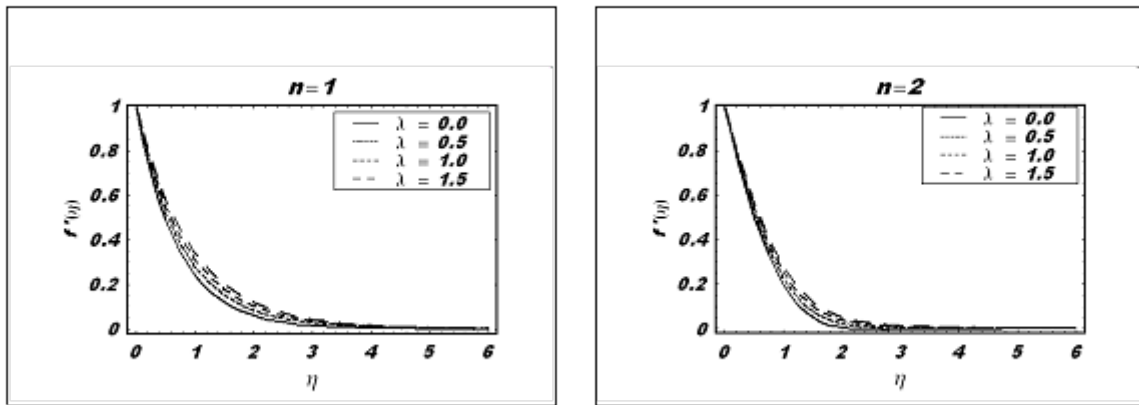


**Figure 7** The influence of the convection parameter,  $\lambda$ , on the velocity profiles when  $Pr = 1$ ,  $\gamma = 1$  and  $M = 1$  are fixed.

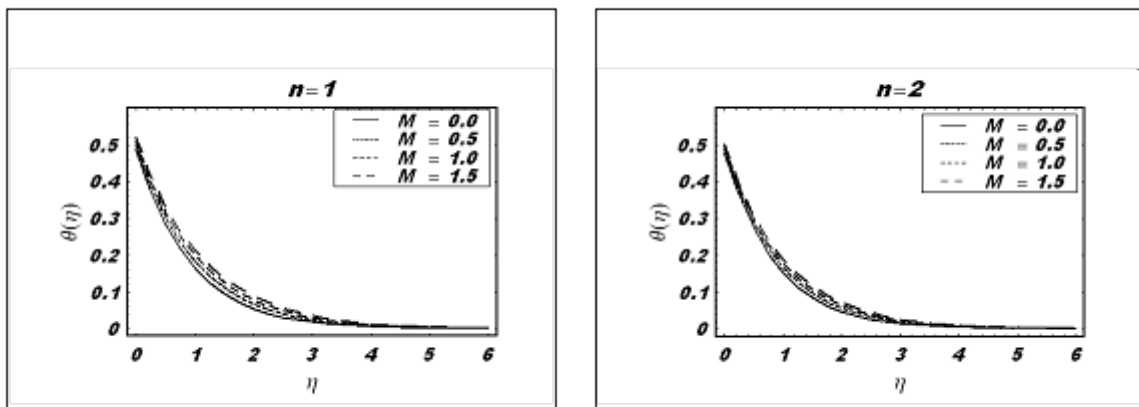


**Figure 8** The influence of the magnetic parameter,  $M$ , on the temperature profiles when  $Pr = 1$ ,  $\gamma = 1$  and  $\lambda = 1$  are fixed.

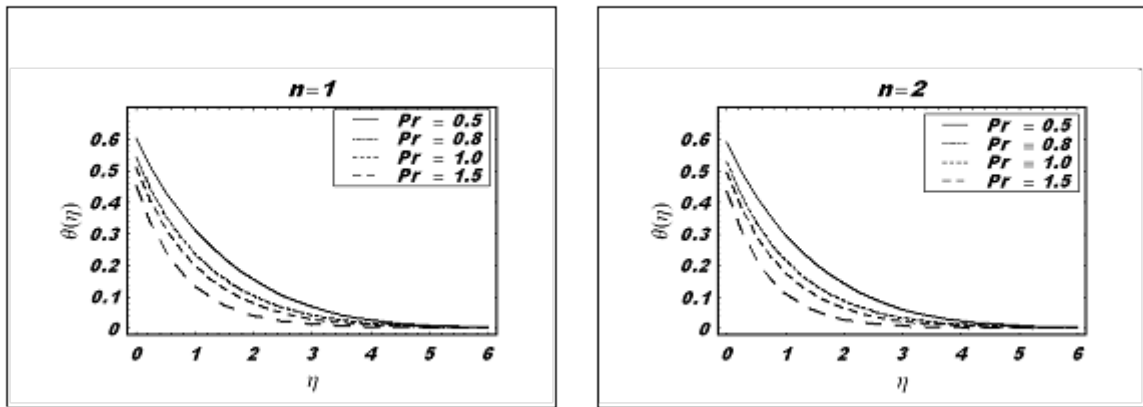


**Figure 9** The influence of the Prandtl number,  $Pr$ , on the temperature profiles when  $\lambda = 1$ ,  $\gamma = 1$  and  $M = 1$  are fixed.

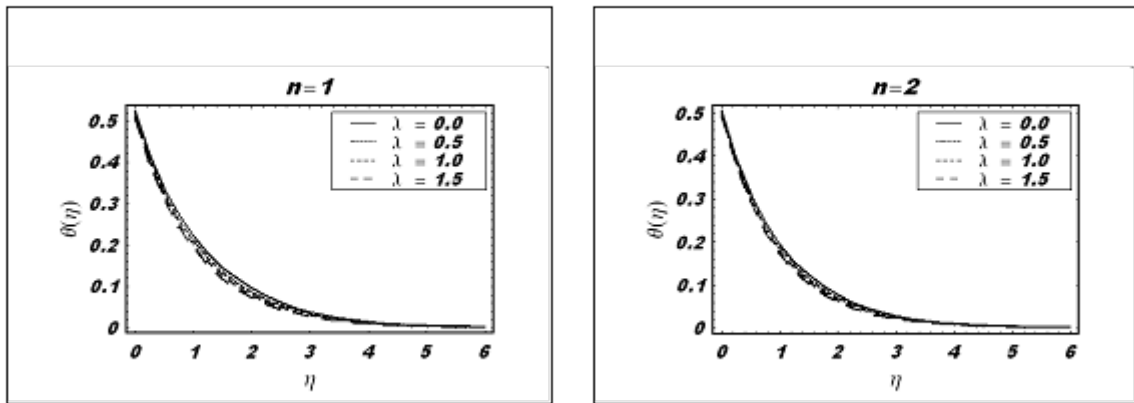


**Figure 10** The influence of the convective parameter,  $\lambda$ , on temperature profiles when  $Pr = 1$ ,  $\gamma = 1$  and  $M = 1$  are fixed.

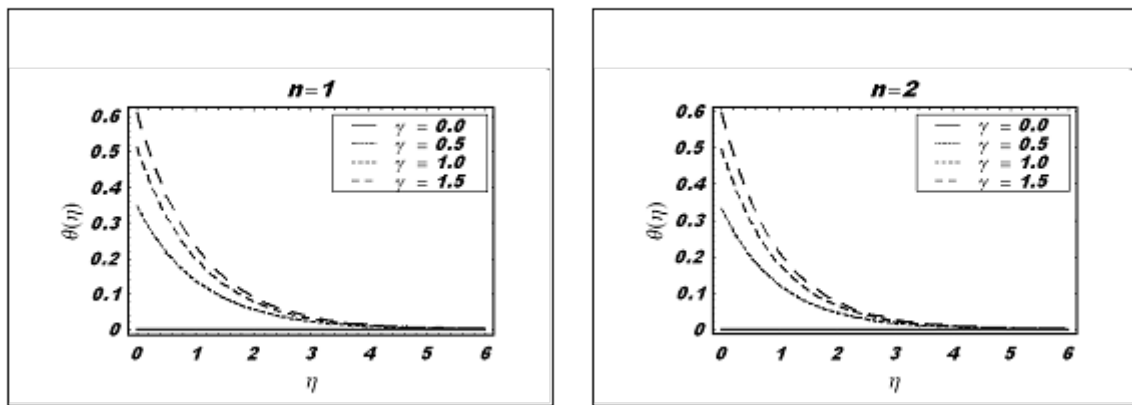


**Figure 11** The influence of the convective parameter,  $\gamma$ , on the temperature profiles when  $Pr = 1$ ,  $\lambda = 1$  and  $M = 1$  are fixed.

**Table 1** The Nusselt number for several sets of values of the different physical parameters.

$\lambda$	Pr	$\gamma$	M	n = 1	n = 2
				$-\theta'(0)$	$-\theta'(0)$
0.0	1	1	1	0.476822	0.495804
0.5	1	1	1	0.483944	0.500763
1.0	1	1	1	0.490044	0.505246
1.5	1	1	1	0.495340	0.509319
1	0.0	1	1	0.230404	0.230405
1	0.5	1	1	0.398300	0.408310
1	1.0	1	1	0.490044	0.505246
1	1.5	1	1	0.539293	0.566804
1	1	0.0	1	0	0
1	1	0.5	1	0.327124	0.334525
1	1	1.0	1	0.490044	0.505545
1	1	1.5	1	0.588817	0.610410
1	1	1	0.0	0.511546	0.521438
1	1	1	0.5	0.500000	0.512602
1	1	1	1.0	0.490044	0.505246
1	1	1	1.5	0.481335	0.498950

## Conclusions

We have studied the MHD flow and heat transfer of a power-law fluid on a vertical stretching sheet using convective thermal boundary conditions. The governing coupled partial differential equation is reduced to non-linear ordinary differential equations by using appropriate similarity transformations. The HAM is used to find the given analytic solutions of the reduced equations for different values of the power-index  $n$ . Briefly it is observed that the physical parameters have significant influences on the velocity and the temperature profiles. We conclude the following from the results and discussion:

1. With an increase in the power-law index  $n$ , the boundary layer thickness decreases.
2. The effects of the material parameters  $M$ , and the Prandtl number  $Pr$ , are the same on the velocity but different in the temperature field.
3. With an increase in the convective parameter  $\lambda$  the boundary layer thickness increases for velocity field while it decreases the thermal boundary layer.

## Acknowledgements

The authors would like to thank the anonymous referees for their valuable comments on the improvement of this work.

## References

- [1] WR Schowalter. The application of boundary layer theory to power law pseudo-plastic: similar solutions. *AIChE Journal* 1960; **6**, 24-8.
- [2] A Acrivos. A theoretical analysis of laminar natural convection heat transfer to non-Newtonian fluids. *AIChE Journal* 1960; **6**; 584-90.
- [3] SY Lee and WF Amen. Similar solutions for non-Newtonian fluids. *AIChE Journal* 1966; **12**, 700-8.
- [4] CJ Cran. Flow past a stretching plate. *Zeitschrift für angewandte Mathematik und Physik* 1970; **12**, 645-7.
- [5] HI Anderson and BS Dandapat. Flow of a power law fluid over a stretching sheet. *Stability Appl. Anal. Continuous Media* 1991; **1**, 339-47.
- [6] KV Parasad, PS Datti and K Vajravelu. Hydromagnetic flow and heat transfer of a non-Newtonian power law fluid over a vertical stretching sheet. *Int. J. Heat and Mass Transf.* 2010; **53**, 879-88.
- [7] A Shahzad and R Ali. Approximate analytic solution for magneto-hydrodynamic flow of a non-Newtonian fluid over a vertical stretching sheet. *Can. J. App. Sci.* 2012; **2**, 202-15.
- [8] D Makinde and A Aziz. Mixed convection from a convectively heated vertical plate to a fluid with internal heat generation. *J. Heat Transfer* 2011; **133**, 122501.
- [9] WA Khan and I Pop. Flow and heat transfer over a continuously moving flat plate in a porous medium. *J. Heat Transfer* 2011; **133**, 0504501.
- [10] VG Fox, LE Erickson and LE Fan. Methods for solving boundary layer equations for moving continuous flat surfaces with suction and injection. *AIChE Journal* 1969; **14**, 726-36.
- [11] D Pal. Combined effects of non-uniform heat source / sink and thermal radiation on heat transfer over an unsteady stretching permeable surface. *Commun. Nonlinear Sci. Numer. Simulat.* 2011; **16**, 1890-904.
- [12] T Hayat, H Zaman and M Ayub. Analytical solution of hydromagnetic flow with Hall effect over a surface stretching with a power-law velocity. *Num. Math. Partial Diff. Eqn.* 2011; **27**, 937-59.
- [13] IA Hassanien, AA Abdullah and RSR Gorla. Flow and heat transfer in a power law fluid over a non-isothermal stretching sheet. *Math. Comput. Model.* 1998; **9**, 105-16.
- [14] HI Anderson, KH Bech and BS Dandapat. Magnetohydrodynamic flow of a power-law fluid over a stretching sheet. *Int. J. Non-Linear Mech.* 1992; **27**, 929-36.
- [15] KV Parasad and K Vajravelu. Heat transfer in the MHD flow of a power law fluid over a non-isothermal stretching sheet. *Int. J. Heat Mass Transf.* 2009; **52**, 4956-65.
- [16] A Aziz. A similarity solution for laminar thermal boundary layer flow over a flat plate with a convective surface boundary condition. *Commun. Nonlinear Sci. Numer. Simulat.* 2009; **14**, 1064-8.
- [17] R Cortell. Suction, viscous dissipation and thermal radiation effects on the flow and heat

- transfer of a power-law fluid past an infinite porous plate. *Chem. Eng. Res. Des.* 2010; **85**, 85-93.
- [18] SJ Liao. A new branch of solutions of boundary layer flows over an incompressible stretching plate. *Int. J. Heat Mass Transf.* 2005; **48**, 2529-39.
- [19] SJ Liao. A short review on the homotopy analysis method in fluid mechanics. *J. Hydrodynamics* 2010; **22**, 882-4.
- [20] T Hayat, M Khan and M Ayub. On the explicit analytic solutions of an Oldroyd 6-constant fluid. *Int. J. Eng. Sci.* 2004; **42**, 123-35.
- [21] TR Mahapatra, SK Nandy and AS Gupta. Analytic solution of magnetohydrodynamic stagnation-point flow of a power-law fluid towards a stretching surface. *Appl. Math. Comput.* 2009; **215**, 1696-710.
- [22] S Abbasbandy. Homotopy analysis method for the Kawahara equation. *Nonlinear Anal. Real World Appl.* 2010; **11**, 307-12.
- [23] PK Rao, AK Sahu and RP Chhabra. Momentum and heat transfer from a square cylinder in power law fluids. *Int. J. Heat Mass Transf.* 2011; **54**, 390-403.